

LETTERS

A photonic quantum information interface

S. Tanzilli¹, W. Tittel¹, M. Halder¹, O. Alibart², P. Baldi², N. Gisin¹ & H. Zbinden¹

Quantum communication requires the transfer of quantum states¹, or quantum bits of information (qubits), from one place to another. From a fundamental perspective, this allows the distribution of entanglement and the demonstration of quantum non-locality over significant distances^{2–6}. Within the context of applications, quantum cryptography offers a provably secure way to establish a confidential key between distant partners⁷. Photons represent the natural flying qubit carriers for quantum communication, and the presence of telecommunications optical fibres makes the wavelengths of 1,310 nm and 1,550 nm particularly suitable for distribution over long distances. However, qubits encoded into alkaline atoms that absorb and emit at wavelengths around 800 nm have been considered for the storage and processing of quantum information^{8–11}. Hence, future quantum information networks made of telecommunications channels and alkaline memories will require interfaces that enable qubit transfers between these useful wavelengths, while preserving quantum coherence and entanglement^{12–14}. Here we report a demonstration of qubit transfer between photons of wavelength 1,310 nm and 710 nm. The mechanism is a nonlinear up-conversion process, with a success probability of greater than 5 per cent. In the event of a successful qubit transfer, we observe strong two-photon interference between the 710 nm photon and a third photon at 1,550 nm, initially entangled with the 1,310 nm photon, although they never directly interacted. The corresponding fidelity is higher than 98 per cent.

Superposition of quantum states and entanglement are the fundamental resources of quantum communication and quantum information processing¹. From an abstract point of view, the nature of the carrying particle is irrelevant since only amplitudes and relative phases are exploited to encode the elementary qubits. Historically, experiments have proved many times that the fascinating properties of quantum correlations can be observed with pairs of photons¹⁵, trapped ions^{12–14}, trapped atoms¹⁶ or cold gases¹⁷. However, the most appropriate carrier and associated encoding observable depend on the specific task. Photons have been proved suitable to transmit quantum information^{18–21}, and atoms or ions to store²² and process^{23,24} it. Photonic entanglement often relies on polarization^{15–18,25}, energy-time²⁶, or time-bin²⁷ coding. Depending on the quantum communication channel, the wavelength of the photonic carrier is also important. The use of telecommunications wavelengths (1,310 and 1,550 nm) is particularly advantageous when employing optical fibres²⁵, while free space transmission is mostly based on shorter wavelengths²⁶.

Future realizations of quantum networks, containing elementary quantum processors and memories, connected by communication channels, require quantum interfaces capable of transferring qubit states from one type of carrier to another. This demands the reversible mapping between photons and atoms, which also includes the mapping between photons of different wavelengths²⁸. However, as opposed to the reproduction of classical information between different media, it is not possible to merely measure the properties

of a given quantum system and replicate them accordingly, as a result of the no-cloning theorem²⁹. Nevertheless, it is possible to resort to a transfer of the quantum information based on an interaction that maintains the coherence properties of the initial quantum system.

In this Letter, we demonstrate a direct quantum interface for photonic qubits at different wavelengths. As illustrated in Fig. 1, an arbitrary qubit carried by a flying telecommunications photon at 1,310 nm (λ_B), initially entangled with a photon at 1,550 nm (λ_A), is coherently transferred to another photon at a wavelength of 710 nm (λ_C) using sum frequency generation (SFG). The final wavelength is close to that of alkaline atomic transitions.

In the following, we first present the theoretical description of our quantum interface. We then recall how to create and characterize maximally energy-time entangled photon pairs. The coherent quantum information transfer, taking advantage of an up-conversion stage, is then introduced. Finally, we show how this operation preserves the initial entanglement by measuring the two-photon interference between the 710 and 1,550 nm photons, and thus we demonstrate a universal qubit transfer.

Consider two systems labelled A (held by Alice), B and B' (held by Bob). In our case these systems are modes of the electro-magnetic field in optical fibres. Initially, B' is in the vacuum state denoted $|0\rangle$, while A and B may be entangled, with Schmidt coefficients c_1 and c_2 :

$$|\Psi\rangle_{AB} = (c_1|a_1\rangle_A|b_1\rangle_B + c_2|a_2\rangle_A|b_2\rangle_B) \quad (1)$$

The pairs of orthogonal states $|a_j\rangle$ and $|b_j\rangle$, $j \in \{1, 2\}$, span Alice and Bob's qubit space, respectively. For example, $|a_j\rangle$ could represent one photon in either the vertical ($j=1$) or horizontal ($j=2$) polarization state, or, as in our case, one photon in the first ($j=1$) or second ($j=2$) time-bin state. The desired state after a successful transfer from B to B' reads:

$$|\Psi\rangle_{AB'} = |0\rangle_A(c_1|a_1\rangle_{B'} + c_2|a_2\rangle_{B'}) \quad (2)$$

Such a transfer is achieved by an interaction described by the effective

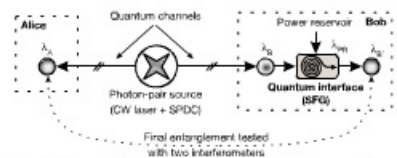


Figure 1 | Schematic illustration of the experiment concept. First, a photon-pair source produces, by spontaneous parametric down-conversion (SPDC), energy-time entangled photons at wavelengths λ_A and λ_B that are sent to Alice and Bob, respectively. Next, the qubit transfer is performed at Bob's location from photon λ_B to photon λ_C using sum frequency generation (SFG). The final entanglement between the newly created photon λ_A and Alice's photon λ_A is tested using the Franson configuration³⁰ (see Fig. 2).

hamiltonian

$$\hat{H} = 1, \otimes g_1 |0\rangle_A |b_1\rangle_B |0\rangle_{B'} + g_2 |0\rangle_A |b_2\rangle_B |0\rangle_{B'} + H.c. \quad (3)$$

where g_1 and g_2 are coupling constants. The evolution can be computed (assuming an interaction time of 1 unit):

$$e^{-i\hat{H}}|\Psi\rangle_{AB} = \cos[g_1]c_1|a_1\rangle_A|b_1\rangle_B|0\rangle_{B'} + \cos[g_2]c_2|a_2\rangle_A|b_2\rangle_B|0\rangle_{B'} + \sin[g_1]c_1|a_1\rangle_A|0\rangle_B|b_1\rangle_{B'} + \sin[g_2]c_2|a_2\rangle_A|0\rangle_B|b_2\rangle_{B'} \quad (4)$$

$$- \sin[g_1]c_2|a_1\rangle_A|b_2\rangle_B|0\rangle_{B'} - \sin[g_2]c_1|a_2\rangle_A|b_1\rangle_B|0\rangle_{B'} \quad (5)$$

Note that in the second terms in equations (4) and (5), the coefficients c_j are multiplied by g_j . This implies that the transfer preserves probability amplitudes and quantum coherence if and only if the two coupling constants are equal, both in amplitude and phase: $g_1 = g_2 = g$. In other words, the transfer can be achieved with perfect fidelity provided this condition is satisfied. In such a case the

evolution simplifies to:

$$e^{-i\hat{H}}|\Psi\rangle_{AB} = \cos[g]c_1|a_1\rangle_A|b_1\rangle_B|0\rangle_{B'} - ig \frac{\sin[g]}{g} |a_1\rangle_A|b_1\rangle_{B'}|0\rangle_B \quad (6)$$

Consequently, the transfer probability is 1 for $|g| = \pi/2$.

Figure 2 presents our two-photon source, S. It consists of a CW pump laser diode with a coherence length L_c exceeding 300 m, attenuated down to a few microwatts at $\lambda_p = 711.6$ nm, and of a quasi-phase-matched periodically poled lithium niobate waveguide^{31,32} (PPLN/W1). The poling period is chosen so as to create down-converted pairs of photons whose wavelengths are centred at 1,312 and 1,555 nm, respectively. After separation at a fibre-optic wavelength division multiplexer (WDM), the 1,555 and 1,312 nm photons are sent to Alice and Bob, respectively, using standard telecommunications optical fibres.

The long coherence length of the pump laser implies that each pump photon has a very well defined energy. Accordingly, the down-conversion process yields pairs of photons that are energy correlated as governed by energy conservation: each photon from a pair has an uncertain energy, uncertain in the usual quantum sense, but the sum of the energies of the two photons from a pair is very well defined. In

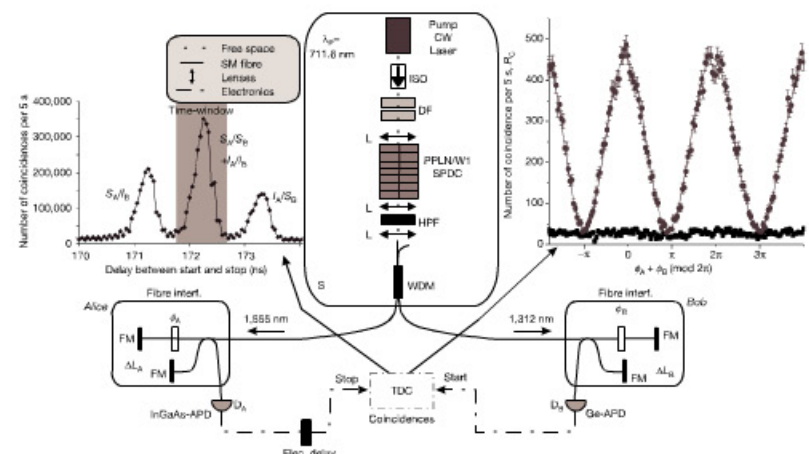


Figure 2 | Experimental Franson-type set-up used for the creation and analysis of energy-time entangled pairs of photons. Alice and Bob's analysers are equally unbalanced Michelson interferometers made of telecommunications optical fibre and Faraday mirrors (FM). The corresponding path length differences are labelled as ΔL_A and ΔL_B , respectively. The source is composed of a CW laser (Topica Photonics DL100), an isolator (ISO), a nonlinear periodically poled lithium niobate (PPLN) waveguide, a wavelength division multiplexer (WDM) and suitable fibre coupling lenses. It also includes a high-pass wavelength filter (HPF) behind the crystal to discard the remaining pump photons, and lenses (L) to couple the created photons into a single mode (SM) fibre. The down-conversion quasi-phase matching is obtained with a specific poling period Λ of 14.1 μm and at a temperature of 85°. This 1-cm-long waveguide features a down-conversion efficiency greater than 10^{-7} . At Bob's location the germanium avalanche photodiode (Ge-APD) (NEC, D9) is liquid nitrogen cooled and passively quenched, while the InGaAs-APD (id Quantique id200, D4) at Alice's location is operated in gated mode. The APDs show quantum

detection efficiencies of about 10% and 14% and probabilities of dark counts of around 3×10^{-5} and 10^{-5} per nanosecond, respectively. The outputs from these APDs provide the start and stop signals for a time-to-digital converter (TDC) that records a coincidence histogram (left inset) as a function of the time difference between its two inputs. This picture is composed of three different peaks, which arise from different combinations of photon transmissions through their respective interferometer, either the short (s) or the long (l) arm. The events where both photons take the same arms (s/s and l/l) are indistinguishable as described by equation (7), leading to photon pair interference. They can be discriminated from the other possibilities (s/l and l/s) by means of a time-resolved coincidence detection. The corresponding coincidence count rate R_C as a function of the combined phase ($\phi_A + \phi_B$) is shown in the right inset. We find sinusoidal interference fringes with more than 97% net visibility. Note finally that the variation of the combined phase is obtained by changing the temperature in Bob's interferometer.

¹Group of Applied Physics, University of Geneva, 1211 Geneva 4, Switzerland. ²Laboratoire de Physique de la Matière Condensée, Université de Nice-Sophia Antipolis, Parc Valrose, 06108 Nice Cedex 2, France.

LETTERS

NATURE [Vol 437] September 2005

NATURE [Vol 437] September 2005

LETTERS

addition, the two photons are also time correlated, as they are emitted simultaneously within their coherence time. However, the emission time of a pair is uncertain within the pump laser coherence. Hence the paired photons are entangled according to the Einstein-Podolsky-Rosen (EPR) paradox²⁴, energy and time replacing the historical position and momentum variables, respectively. More precisely, the processes of photon-pair creation at different times separated by Δt are coherent as long as $\Delta t \ll C_p/c$. The underlying quantum coherence of the photon pairs therefore comes from the pump laser itself.

In order to reveal and characterize the coherence carried by these energy-time entangled photon pairs we perform a Franson-type experiment²⁵ and infer the degree of entanglement from the measured two-photon interference visibility. For this purpose the two photons are sent to two analysers, one on Alice's and the other on Bob's side, that consist, in our case, of unbalanced Michelson interferometers made from standard telecommunications, fibres, fibre-optic beam splitters, and Faraday mirrors (Fig. 2). To prevent single photon interference, the optical path length difference in each interferometer (ΔL_A and ΔL_B , respectively) has to be much greater than the coherence length of the single photons, $C_p \approx 150 \mu\text{m}$, deduced from the 15 nm spectral bandwidth of the down-converted light. Each single photon therefore has an equal probability of $\frac{1}{2}$ to exit at one of the outputs of its analyser. Moreover, to maximize two-photon interference, these analysers have to be equally unbalanced, $\Delta L_A = \Delta L_B = \Delta L$, within the coherence length of the single photons.

At the same time, however, since an entangled pair represents the quantum object to be analysed, both ΔL values ($\sim 20 \text{ cm}$ in our case) have to be much smaller than the coherence length of the pair which is given by the pump laser ($C_p > 300 \text{ m}$).

At the output of each interferometer, the single photons are detected. Using a time-resolved coincidence detection between Alice and Bob as depicted in Fig. 2, we can post-project the initial energy-time entangled state onto a time-bin entangled state of the form:

$$|\Psi\rangle_{\text{post}} = \frac{1}{\sqrt{2}} (|s_A, s_B\rangle + e^{i\phi_A + \phi_B} |l_A, l_B\rangle) \quad (7)$$

where ϕ_A and ϕ_B are phases associated with the path length difference ΔL_A and ΔL_B of the related interferometers. The state given by equation (7) corresponds to the events where the down-converted photons both travel through the same arms of the interferometers, that is, s_A, s_B or l_A, l_B , these two possibilities being indistinguishable. Thus, varying the combined phase ($\phi_A + \phi_B$), we observe sinusoidal interference fringes in the coincidence rate with net (accidental coincidences discarded) and raw visibilities of $97.0 \pm 1.1\%$ and $87.4 \pm 1.1\%$, respectively (see Fig. 2). Because almost all accidental coincidences are due to detector dark counts, the purity of the created state, and hence the performance of the source, should be characterized by the net visibility. As this figure of merit is very close to the 100% predicted by quantum theory, we conclude that our source provides a state close to a pure maximally

entangled state, in particular, suitable to violate the Bell inequalities²⁶. Note that the missing 3% in the net visibility is most probably due to the measurement technique rather than the state preparation¹.

Now that we have characterized our entanglement resource, we proceed to the quantum information transfer, that is, the transfer of the qubit carried by Bob's particle to another photon of shorter wavelength. To this end, we replace the fibre-optic interferometer and the germanium avalanche photodiode (Ge-APD) on Bob's side by another nonlinear PPLN waveguide (PPLN/W2), a bulk-optic Michelson interferometer, and a silicon avalanche photodiode (Si-APD), as depicted in Fig. 3. This second nonlinear crystal, together with a power reservoir (PR) consisting of a CW coherent laser at $\lambda_{\text{PR}} = 1,560 \text{ nm}$ and an erbium-doped fibre amplifier (EDFA), serves as an up-conversion stage for the incoming 1,312 nm photons produced by the previously described source. As a result of this operation, which is the opposite process to down-conversion, photons at 1,312 and 1,560 nm are annihilated and photons at 712.4 nm are created on Bob's side. The coherence of the PR directly relates to the phase difference between the coefficients in the effective hamiltonian of equation (3): $g_1 = \xi(t_1)$ and $g_2 = \xi(t_2)$ where $\xi(t)$ is proportional to the PR electric field at times t_1 and t_2 , respectively. The quantity $\alpha(t_1 - t_2)$ corresponds to the imbalance of the interferometers, using the notation of equation (7). The previous general condition $g_1 = g_2$ of equation (6) therefore translates, in the case at up-conversion, as a constraint on the PR's coherence: $C_p^{\text{PR}}/c \gg t_1 - t_2$. In our experiment this condition is definitely satisfied as $C_p^{\text{PR}} > 1 \text{ km}$, which is clearly much greater than the 20 cm path length difference of Bob's analyser. Accordingly, the resulting photons at λ_B should become entangled with Alice photons at λ_A , although they never directly interacted.

The PR delivers 700 mW in a standard telecommunications fibre. We measured, with classical fields, an internal up-conversion efficiency of 80% per watt of reservoir power at optimum phase-matching²⁷⁻²⁹. Note that this value is underestimated, as the losses in the waveguide itself are neglected. This up-conversion efficiency decreases by a factor of 2 when changing the single photon wavelength by $\pm 1 \text{ nm}$. Taking advantage of the energy correlation between the photons of a pair, we reduced the bandwidth by filtering the spectrum of the photons at 1,555 nm travelling to Alice to 1.5 nm (BPF_A) and increased the power of the source pump laser in order to have a reasonable photon-pair production rate in this bandwidth. Hence, the overall up-conversion probability is only limited by the available pump power and coupling losses between the waveguide and single mode optical fibres at input and output faces. From this classical conversion efficiency, taking into account the reservoir power, a realistic 40% coupling efficiency into the waveguide (both for the PR and the qubit to be transferred) and the ratio between the initial and final wavelengths, we estimate the probability of a successful quantum information transfer to be: $P_{\text{success}} = 80\% \times 0.7 \times 0.4 \times (0.4)^2 \times \frac{1,560}{1,312} \approx 5\%$. Let us mention that indirect qubit transfer can also be achieved via teleportation²⁴; however, in contrast to teleportation, quantum information transfer is achieved with a much higher success probability.

After the up-conversion stage, the 712.4 nm photons enter the temperature stabilized bulk-optic Michelson interferometer. At the output port of this analyser they are coupled, for optimal mode overlap, into a single-mode fibre adapted to visible light with a corresponding coupling efficiency greater than 60%. Then, these photons are sent to the Si-APD (D_B). In order to avoid pollution of the detector by the huge flow of PR photons at 1,560 nm, about 5×10^7 photons per ns, we use a bandpass filter centred at 712 nm (BPF_B, $\Delta\lambda = 10 \text{ nm}$, more than 30 dB attenuation around 1,550 nm), as depicted in Fig. 3. We also take advantage of the combination of poor coupling and guidance of the 1,560 nm reservoir photons in the visible single mode fibre, and of the fact that Si-APDs are essentially insensitive at this wavelength. Then, the electronic signal from this APD triggers the detector of the 1,555 nm photons that arrive on

Alice's side (InGaAs-APD) previously introduced and operated in gated mode). Finally, we record the coincidence events between these two detectors and measure the transfer fidelity.

Figure 3 shows the interference pattern of the coincidence events as a function of the combined phase ($\phi_A + \phi_B$) obtained with our time-resolved coincidence detection. We observe a sinusoidal oscillation with net and raw visibilities of $96.2 \pm 0.4\%$ and $86.4 \pm 0.4\%$, respectively, representing a clear signature of the preserved coherence during the quantum information transfer. The net visibility V_{net} is again very close to the 100% predicted by quantum theory. Assuming that the entire reduction of this visibility can be attributed to an imperfect quantum state transfer, we find a fidelity $F = \frac{1+V_{\text{net}}}{2} \approx 98.5\%$. Note however that this estimation is very conservative since the visibility observed before transfer (see Fig. 2) is hardly higher.

Note that the quantum interface demonstrated in this Letter is not limited to the specific wavelengths chosen. Indeed, suitable modifications of phase-matching conditions and pump wavelengths enable tuning to any desired wavelengths. In particular, it allows mapping of telecommunication photonic qubits onto qubits encoded at a wavelength corresponding to alkaline atomic transitions. It is particularly interesting to take advantage of periodically poled waveguiding structures, as employed here. First, phase matching conditions can easily be tuned over a broad range by changing the grating period. Second, these components yield very high up- and down-conversion efficiencies^{28,29}. This permits the use of a modest reservoir power to achieve a reasonable qubit transfer probability. In the case of applications requiring very narrow photon bandwidths, for instance when transferring quantum information onto atoms³⁰, bright down-converters make very narrow spectral filtering possible while maintaining high photon-pair creation rates with reasonable pump powers. In addition, the narrow filtering ensures optimal phase-matching over the whole bandwidth of the photons to be up-converted, hence maximizing this process.

In this work we demonstrated, in the most general way, a direct quantum information interface between qubits carried by photons of widely different wavelengths. To this end, we verified that entanglement remains unaffected, even though one of the two entangled photons is submitted to a wavelength up-conversion process. This interface may find applications in quantum networks, where mapping of travelling qubits (for example, qubits encoded onto telecommunication photons, and stationary atomic qubits featuring resonance at much shorter wavelengths) is necessary.

Received 27 May; accepted 7 July 2005.

1. Tittel, W. & Vuckovic, G. Photonic entanglement for fundamental tests and quantum communications. *Quant. Inform. Comput.* **1**, 3-56 (2001).
2. Tittel, W., Brendel, J., Zbinden, H. & Gisin, N. Violation of Bell inequalities by photons more than 10 km apart. *Phys. Rev. Lett.* **81**, 3563-3566 (1998).
3. Marcik, J. et al. Distribution of time-entangled qubits over 50 km of optical fiber. *Phys. Rev. Lett.* **93**, 180502 (2004).
4. Vuckovic, G., Jermolenko, T., Simon, C., Vuckovic, H. & Zehner, A. Violation of Bell's inequality under strict Einstein locality conditions. *Phys. Rev. Lett.* **81**, 5039-5043 (1998).
5. Resch, K. J. et al. Distributing entanglement and single photons through an intra-city, free-space quantum channel. *Opt. Express* **13**, 202-209 (2005).
6. Peng, C.-Z. et al. Experimental free-space distribution of entangled photon pairs over a noisy ground atmosphere of 13 km. *Phys. Rev. Lett.* **94**, 150501 (2005).
7. Gisin, N., Ribordy, G., Tittel, W. & Zbinden, H. Quantum cryptography. *Rev. Mod. Phys.* **74**, 145-195 (2002).
8. Blinov, B. B., Moehring, D. L., Duan, L.-M. & Monroe, C. Observation of entanglement between a single trapped atom and a single photon. *Nature* **428**, 153-157 (2004).
9. Uhlir, S., Shafir, M. S., Shapiro, J. H. & Hemmer, P. R. Long distances, unconditional teleportation of atomic states via complete Bell state measurements. *Phys. Rev. Lett.* **87**, 167903 (2001).
10. Huang, J. & Kumar, P. Observation of quantum frequency conversion. *Phys. Rev. Lett.* **68**, 2153-2156 (1992).
11. Mülken, P., Gisin, G. & De Martini, F. Frequency hopping in quantum interferometry. *Fortsch. Phys.* **51**, 435-441 (2003).
12. Rowe, M. A. et al. Experimental violation of a Bell's inequality with efficient detection. *Nature* **409**, 791-794 (2001).

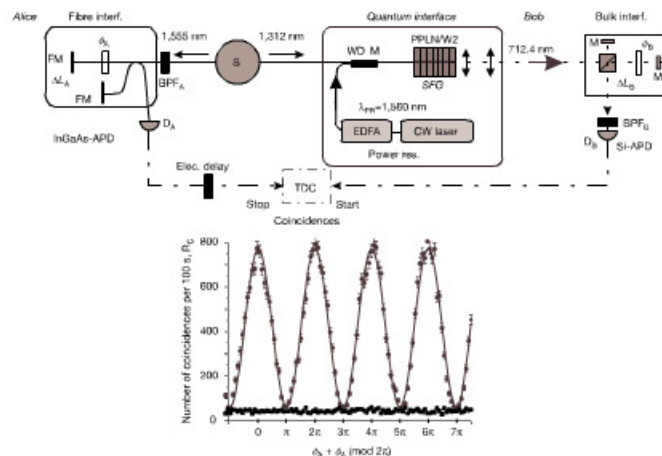


Figure 3 | Experimental set-up for the coherent transfer of quantum entanglement. On Bob's side, PPLN/W2, pumped by a high-coherence CW 700 mW power reservoir at 1,560 nm (laser 8168A from HP + EDFA from Keopsys), ensures the transfer of the qubit from 1,312 to 712.4 nm via the up-conversion process. This second 1-cm-long PPLN waveguide is of the same kind as that used for the down-conversion. They were both fabricated using the technique of soft proton exchange³¹, and feature almost identical phase-matching conditions. Both 1,312 and 1,560 nm wavelengths are mixed at a second WDM whose output port is directly butt-coupled to the input face of PPLN/W2 without any additional optics. At the output of the waveguide, the newly created photons at 712.4 nm are coupled into a single mode fibre and detected using a silicon avalanche photodiode (EG&G AQ-141-FC, D_B). The coherence of the transfer is verified by measuring photon-pair interference between the 712.4 and 1,555 nm photons in the Franson configuration. The analysis on Bob's side utilizes an unbalanced, bulk-optic interferometer that is aligned with respect to Alice's. Although the coincidence rate is substantially reduced owing to a limited up-conversion probability and losses in the interferometers, the analysis of the coincidence events yields interference fringes with net and raw visibilities of 96 and 86%, respectively. This confirms the previously obtained result without the quantum interface and demonstrates, in the most general way, coherent transfer of quantum information between two photons.